Original scientific paper
https://doi.org/10.33180/InfMIDEM2024.104

Informacije MIDEM
Journal of Microelectronics,
Electronic Components and Materials
Vol. 54, No. 1(2024), 39 – 49

Hexagonal Convolutional Neural Network for Noma Rician Channel Estimator using Hexagonal Quadrature Amplitude Modulation

Mohan Dhas Jenish Dev[1], David Judson[2]

[1]Assistant professor, department of Electronics and Communication Engineering, Cape Institute of technology, Rajakrishnapuram, Tamil Nadu, India
[2]Associate professor, Department of Electronics and Communication Engineering, St. xaviers catholic college of Engineering, Chunkankadai, Nagercoil, Tamil Nadu, India

Abstract: NOMA techniques have attracted much attention due to their ability to support massive connectivity, heterogeneous data traffic, and ultra-low latency requirements, making them ideal for next-generation wireless communication networks. In this paper proposed a novel Hexa CNN for NOMA Rician channel estimator using Hexagonal Quadrature Amplitude Modulation for signal detection and channel estimation (Hexa-QAM). Conventional OFDM-NOMA with HQAM is utilized at the transmitter (tx) side as pilot symbols which inserted to OFDM-NOMA signals to employs the channel estimation (CE) and signal detection advantages of OFDM. Three pilot insertion types Comp, Block, and Hexa were used in the proposed model. The proposed Hexa-QAM can detect the symbols for all users without additional operations based on pilot responses and data signals. However, Hexa CNN is used at the receiver to accomplish a joint flexible signal detection. The Hexagonal Quadrature Amplitude Modulation (Hexa CNN) achieves much better error performance than similar detectors. The Energy Efficiency of the proposed Hexa-QAM technique is 17%, 18%, 23.2%, 23% and 28% better than existing techniques. The accuracy of the proposed technique can be as high as 99.95%, while that of traditional models like the OMA-NOMA, MRC, PD-NOMA and UR-NOMA is 84.9%, 87.58%, and 93.91%, respectively.

Keywords: Orthogonal Frequency Division Multiplexing; Convolutional neural network; Hexagonal Quadrature Amplitude Modulation; Non-Orthogonal Multiple Access

Šestkotno konvolucijsko nevronsko omrežje za ocenjevanje kanala Noma Rician z uporabo šestkotne kvadraturne amplitudne modulacije

Izvleček: Tehnike NOMA so pritegnile veliko pozornosti zaradi svoje zmožnosti podpiranja množične povezljivosti, heterogenega podatkovnega prometa in zahtev po izjemno nizki zakasnitvi, zaradi česar so idealne za brezžična komunikacijska omrežja naslednje generacije. V tem članku je predlagana nova Hexa CNN za ocenjevanje kanala NOMA Rician z uporabo heksagonalne kvadraturne amplitudne modulacije za zaznavanje signalov in ocenjevanje kanala (Hexa-QAM). Konvencionalni OFDM-NOMA s HQAM se uporablja na strani oddajnika (tx) kot pilotni simboli, ki se vstavijo v signale OFDM-NOMA, da se uporabijo prednosti OFDM za ocenjevanje kanala (CE) in zaznavanje signalov. V predlaganem modelu so bili uporabljeni trije tipi vstavljanja pilotnih simbolov: Comp, Block in Hexa. Predlagani Hexa-QAM lahko zazna simbole za vse uporabnike brez dodatnih operacij na podlagi pilotnih odzivov in podatkovnih signalov. Vendar se Hexa CNN uporablja pri sprejemniku, da se doseže skupno prožno zaznavanje signalov. Šestkotna kvadraturna amplitudna modulacija (Hexa CNN) dosega veliko boljšo učinkovitost napak kot podobni detektorji. Energetska učinkovitost predlagane tehnike Hexa-QAM je za 17%, 18%, 23,2%, 23% in 28% boljša od obstoječih tehnik. Natančnost predlagane tehnike je lahko kar 99,95%, medtem ko je natančnost tradicionalnih modelov, kot so OMA-NOMA, MRC, PD-NOMA in UR-NOMA, 84,9%, 87,58% oziroma 93,91%.

Ključne besede: multipleksiranje ortogonalnih frekvenc; konvolucijska nevronska mreža; šestkotna kvadraturna modulacija amplitude; neortogonalen dostop

** Corresponding Author's e-mail: jenishdev56@outlook.com*

How to cite:
M. D. J. Dev et al., "Hexagonal Convolutional Neural Network for Noma Rician Channel Estimator using Hexagonal Quadrature Amplitude Modulation", Inf. Midem-J. Microelectron. Electron. Compon. Mater., Vol. 54, No. 1(2024), pp. 39–49

1 Introduction

OFDM (Orthogonal Frequency Division Multiplexing) is a wireless communication modulation technology used to transmit multiple messages over the same band [1]. Multiple orthogonal subcarrier signals with overlapping spectra are delivered in close proximity, with each carrier modulated with bits from the incoming stream to allow multiple bits to be transmitted in parallel [2]. Signal is modulated at a low symbol rate utilizing a standard modulation approach. This retains total data rates comparable to standard single-carrier modulation approaches in the same bandwidth [3].

A multiple access technique called NOMA enables several users to share the same time-frequency resources without interfering with one another's broadcasts [4]. This enables more users to be served with the same amount of bandwidth, making it a viable solution for future wireless communication systems [5]. The ability of NOMA to serve a high number of users while sharing the same time and frequency resources is the primary reason for its implementation in 5G [6]. It provides excellent device performance, efficiency, expanded coverage, low latency, and massive networking [7,8].

CE techniques for OFDM frames based on pilot action plans are under investigation [9,10]. The pilot insertion action plan affects the CE, which is considered in several calculations for both channel evaluation at pilot frequency and channel insertion [11,12]. At the pilot frequency, the channel is estimated using LS and LMS, and the channel is inserted using direct interleaving, which includes a second request, low-pass representation, cubic spline interleaving, and additional spatial timing. [13,14]. Proposed a novel Hexa CNN for NOMA Rician channel estimator using Hexagonal Quadrature Amplitude Modulation for signal detection and CE. The major contribution of the work has been followed by:

- Conventional OFDM-NOMA with HQAM is used on the tx side as pilot symbols that are incorporated into OFDM-NOMA signals to take use of OFDM's CE and signal detection capabilities.
- Three pilot insertion types Comp, Block, and Hexa were used in the proposed model. The proposed Hexa-QAM can detect the symbols for all users without additional operations based on pilot responses and data signals.
- However, Hexa CNN is used at the receiver to accomplish a joint flexible signal detection. The Hexagonal Quadrature Amplitude Modulation (Hexa CNN) achieves much better error performance than similar detectors.

The remaining portion of the work has been followed by Section 2 denotes the literature survey Section 3 denotes the proposed Hexa-QAM methodology 4 denotes the Result and Discussion and the closing remarks are illustrated in section 5

2 Literature review

Recently, a lot of research has been done to address CE in OFDM-NOMA. This section explains the most recent techniques used in this domain.

In 2021 Hadi, M. and Ghazizadeh, R., [15] Created an OMA-NOMA-based approach where the whole bandwidth is split between OMA- and NOMA-based subcarriers to minimize cross-level interference. Simulation results show that in terms of global information throughput performance, the suggested version outperforms the other strategies indexed. In order to optimize the overall cost of an OMA-NOMA-based system, a non-convex optimization problem is developed in which the channel state information (CSI) is not fully understood.

In 2021 Rahdari, F., et al., [16] presented a method that is both easy to use and almost ideal for classifying users in an OFDM-NOMA system. Simulated data indicates that when the variance rises, energy consumption increases more when the distance varies than when the power demand does. One of the most important aspects of such integration, particularly for multimedia communications, is ensuring quality of experience for all connected users.

In 2021 Belmekki, B.E.Y., et al., [17] suggested a maximum ratio combining (MRC) in cooperative VCs transmission systems at road crossings with NOMA. Based on our findings, we determined that using MRC and NOMA is always helpful, even if it means adding complexity to the implementation. Furthermore, 50 percent of all collisions occur at road intersections, making them essential places.

In 2021 Anh, L.T. and Kong, H.Y., et al., [18] developed a power-area (PD-NOMA) system for several users via Nakagami-m fading channels in a multiple energy harvesting (EH) relay networks with hazardous backhaul lines. According to these results, the suggested PD-NOMA machine performs better in terms of customer fairness than the standard orthogonal more than one-get right of entry (OMA) machine. Current concerns include the need for enhanced a high data rate, low latency, network capacity, coverage, and QoS services, which have not been adequately handled.

In 2021 Cogen, F. and Aydin, E., et al., [19] created HQAMQSM, an HQAM assisted QSM approach. In com-

parison to QSM using the QAM scheme, the suggested HQAM-QSM system utilizes less transmission power while offering equal error performance at high SNR. Based on what computer models have shown. Regrettably, battery technology has not advanced as quickly as modern communication technologies. With respect to next-generation communication systems, energy efficiency has become a critical consideration for the reasons mentioned above.

In 2021 Tian, Y., et al., [20] developed for cooperative uplink networks, the opportunistic NOMA (UR-ONOMA) method based on user relay (AF) amplification and propagation aims to appropriately increase the coverage of high-quality services. Numerical results demonstrate that when remote users have weak channels, the developed UR-ONOMA cooperation outperforms NOMA in terms of error probability and throughput when user relays are not used. Peripheral users located distant from the receiver may encounter peripheral interference and may not be supplied if the transmission channels are really weak, which is one of the drawbacks of ordinary NOMA in the electrical domain.

In 2021 Kazemian, M., et al., [21] proposed an E-NOMA to improve the performance of standard FFT-NOMA in 5G networks. According to simulation findings, the proposed E-NOMA approaches outperform FFT-NOMA in terms of PAPR and BER by around 4.3 dB and 9.5 dB. Furthermore, computational complexity is reduced by at least 56% as compared to a NOMA technique based on SLM NOMA has been identified as a promising method for meeting the rising traffic needs of heterogeneous wireless networks.

In 2021 Ghous, M., et al., [22] Created a MIMO-NOMA cooperative transmission strategy with SWIPT support, which included beam-forming and self-interference. Since data rate fairness and outage performance of cell-edge users are critical challenges in MIMO-NOMA systems, we focus on how to resolve these difficulties. To ensure the correctness of our study, we evaluate the analytical expressions using simulations. We demonstrate how employing antenna diversity at the MIMO-NOMA model near and far end terminals improve the outage performance of cell-edge users.

In 2023 Wang, Z., et al., [23] provide an OFDM system built using carrier frequency offset (CFO) models based on DL. Peer evaluations show that DL-based models can work well for large classes of channels without further training if they are trained with the worst (heaviest) multi-pass channel model. However, the carrier frequency offset between the transmitter and the receiver must be correctly estimated due to the OFDM system's sensitivity to carrier frequency offset.

In 2020 Lemayian, J. P., & Hamamreh, J. M et al., [24] suggested an advanced revolutionary small-scale NOMA communication strategy based on physical layer security (PLS) to improve security and reliability for two users. The results show that the proposed model offers less complicated, secure, and efficient communication, making it ideal for applications with low power consumption and restricted computation. Furthermore, according to, the NOMA Energy Domain is no longer a development item in the 3rd Generation Partnership Project (3GPP) and has been deleted from Release 17 due to certain performance degradation problems.

However various literature surveys had been proposed, yet they face challenges like high bit error rate, low energy efficiency, and spectrum efficiency in the system. To overcome these challenges, proposed a novel HEXA-QAM for NOMA Rician channel estimator using Hexagonal Quadrature Amplitude Modulation for signal detection and CE.

3 Proposed RICH-NOMA methodology

In this paper proposed a novel Hexa CNN for NOMA Rician channel estimator using Hexagonal Quadrature Amplitude Modulation for signal detection and channel estimation (Hexa-QAM). OFDM-NOMA signals with inserted pilot symbols are sent to all users via the Rician fading channel. In this research, we employed comb-type, block-type, and Hexa-type pilot insertions1, which are three of the most used forms of pilot designs for CE. Based on pilot answers and data signals, the proposed Hexa-QAM can recognize symbols for all users with no further processes. The Hexagonal Quadrature Amplitude Modulation (Hexa CNN) achieves much better error performance than similar detectors.

3.1 Conventional OFDM-NOMA

Traditional OFDM model use an inverse discrete Fourier transform (IDFT) to transform SC symbols independently of pilot insertion after they are serialized and parallelized. Therefore, the symbols for OFDM-NOMA are provided as follows:

$$a(m) = IDFT\left\{a^{(P)}\right\} = \sum_{P=1}^{M_c} a^{(P)} w^{i(2\pi Pm/M_c)}$$

$$\text{M=1,2...,} M_c \tag{1}$$

Here, the SC symbol stream *a(m)* is before the IDFT. Ns is the frequency domain subcarrier number. In other words, it is the symbol *a(p)* of the k-th OFDM subcar-

rier. To prevent intercarrier interference (ICI) between OFDM subcarriers, According to CP, an OFDM symbol is represented as:

$$a_{CP}(m)=\begin{cases}a(M_s+m), m=-M_{cp},-M_{cp}+1,\ldots,-1\\ a(m), m=1,\ldots M_c,\end{cases} \quad (2)$$

Here, the length of CP is represented by M_{cp}.The CP-added OFDM signal is serialized and transmitted on a Rician fading channel. As a result, the user received the following signal:

$$b_{CP_j}(m)=\sqrt{TA_{CP}(m)\otimes g_j(m)+v_j(m)}$$
$$j=1,2,\ldots M, \quad (3)$$

Initially, the received signal is transformed from serial to parallel at the receiver in eqn (3), and CP is eliminated.

$$b_i(m)=b_{CPi}(m+M_{CP}), \quad m=1,2,\ldots,M_c \quad (4)$$

After removing the CP, the received signal undergoes a discrete Fourier transform (DFT), followed by (4) to convert the signal to serial format.

$$A_j(P)=DFT\{B_j(m)\}=\frac{1}{M_c}\sum_{m=1}^{M_c}B(m)w^{i(2\pi Pm/M_c)},$$

P=1, 2,…, M_c (5)

The signals in (5) are equalized according to the CSIR (eg, complete channel estimate and/or estimated channel).

$$A_j(P)=\frac{B_j(P)}{G_j(P)}, P=1,2,\ldots,M_c \quad (6)$$

In which G_j represents G_j s DFT. The UEN sign makes use of a most probability detector, or MLD, to expect its very own alerts due to the fact it's miles given extra power. Prior to predicting their very own alerts, different UEs execute iterative SIC(s). All UEs' detection estimates and diagnosed symbols are indexed as [5].

$$\hat{A}_j=\underset{l}{\operatorname{argmin}}\left|A_j^{(M-j+1)}-\sqrt{T\alpha_j g_j A_j,l}\right|^2$$

l=1,2,. . . ,N, (7)

$$\hat{A}_j=\underset{l}{\operatorname{argmin}}\left|A_j^{(M-i+1)}-\sqrt{T\alpha_j g_j A_j,l}\right|^2$$

l=1,2,. . . ,N, (8)

where $A_{j,p}$ illustrates estimated symbol of UEi and $\hat{A}_j$ is illustrated in the constellation map. Proposed Hexa-QAM shown in Figure 1.

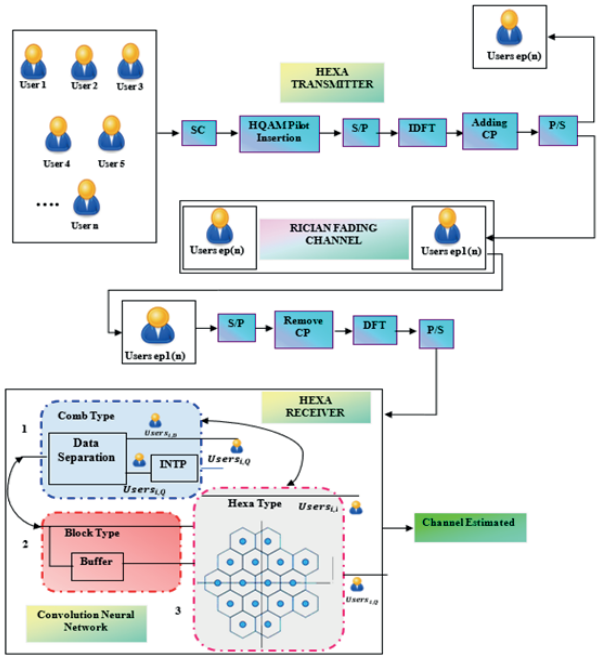

Figure 1: Proposed Hexa-QAM

3.2 Hexa transmitter & receiver

The cyclic prefix (CP) is eliminated from the received signal at the receiver following its conversion to parallel form. DFT is used to restructure the residual signal, which is subsequently transferred to serial format. Consequently, in order to retrieve two successive OFDM signals plus a data symbol (User(i,D)) at the receiver, a buffer must be utilized. Consequently, a comb interpolation approach may be employed to get a priori knowledge of the channel response of the subcarriers carrying the data symbols, allowing for the acquisition of the whole channel frequency response at each subcarrier location. One interpolation block (INTP) shapes Users(i,P). The rebuilt users (i, P) and users (i, D) are fed into his Hexa-CNN network after the INTP block.

3.2.1 Rician fading channel

Another statistical version that makes the idea that the sign includes components a robust LOS element and a random element is the Rician fading version. The linear course with regular amplitude and segment that runs from the Tx to the Rx is called the LOS element.

$$P=\frac{u^2}{2\sigma^2} \quad (9)$$

$P = \frac{u^2}{2\sigma^2}$ described as the scale parameter and Ratio of power contributions from line-of-sight paths to other multipaths. The second one, which serves as a scaling factor for the distribution, Ω is the total power from both paths:

$$\Omega = u^2 + 2\sigma^2 \tag{10}$$

$\Omega = u^2 + 2\sigma^2$ described as the total power obtained across all routes. The function of probability density is

$$u^2 = \frac{P}{1+P}\Omega \tag{11}$$

$$\sigma^2 = \frac{\Omega}{2(1+P)} \tag{12}$$

$$f(a \mid u, \sigma) = \frac{a}{\sigma^2} exp\left(\frac{-\left(a^2+u^2\right)}{2\sigma^2}\right) I_0\left(\frac{au}{\sigma^2}\right) \tag{13}$$

This leads to the following probability density function:

$$f(a) = \frac{2(P+1)a}{\Omega}\exp\left(-P - \frac{(P+1)a^2}{\Omega}\right) I_0\left(2\sqrt{\frac{P(P+1)}{\Omega}}a\right) \tag{14}$$

In this case, I_0 is the first-kind modified Bessel function of order zero at 0th order.

3.3 Hexa pilot insertion

The pilot pattern is the location where the pilot is inserted in the OFDM symbol's frequency and time domains. A suitable pilot pattern can improve communication quality and significantly lower CE error. Figure 2 depicts the pilot insertion signals, with occupied circles representing pilot signals and empty circles representing data symbols. Figure 2 (a) represents the Block type, Figure 2 (b) represents the Comb type, Figure 2 (c) represents the Hexa type.

3.3.1 Block type

According to the first model, pilots are placed into each subcarrier of a single OFDM symbol within a specific time frame. Block-type channels can be used when they fade slowly; that is, when the channel remains stationary for a predetermined amount of OFDM symbols. In case the channel noise W is uncorrelated and the time domain channel vector is Gaussian, the frequency domain MMSE estimate may be obtained as follows:

$$H_{MMSE} = HG_{rX}R_{XX}^{-1}X \tag{14}$$

Where G_{rX} and R_{XX}^{-1} are the cross-covariance matrix between r and X and the auto-covariance matrix of X respectively. R_{XX}^{-1} is the auto-covariance matrix of hand σ2 represents the noise variance E{|W(k)|2}. The LS estimate, which minimizes $(X - YHr)^H (X - YHr)$ is represented by:

$$H_{LS} = Y^{-1}X \tag{15}$$

When the channel is slowly fading, the channel estimation inside the block can be updated using the decision feedback equalizer at each sub-carrier.

3.3.2 Comb type

In the hybrid-type MIMO-OFDM driver model, the drivers are fed into a set of subcarriers in OFDM notation, with interpolation determining the remaining subcarrier channels. When the channel is fast falling, this form

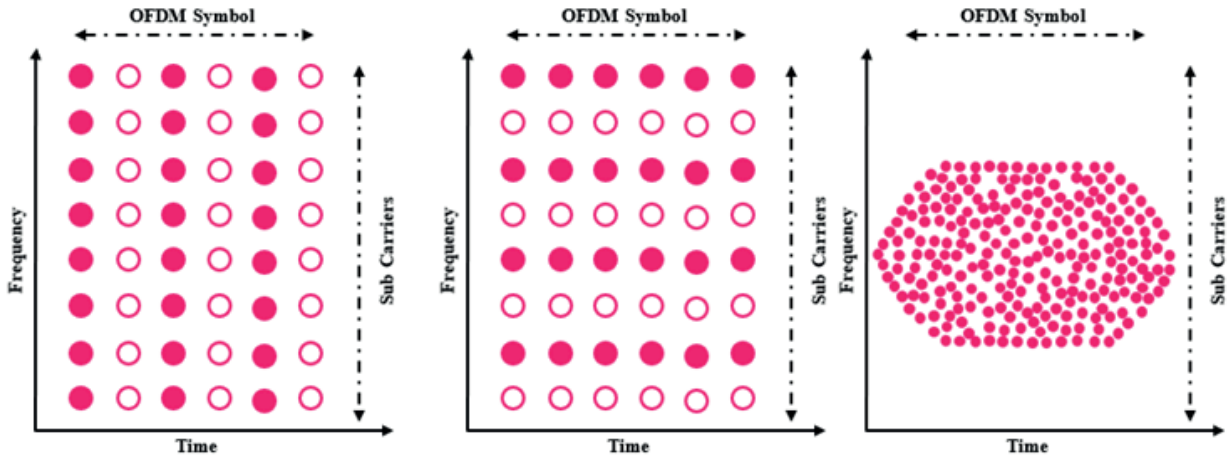

(a) (b) (c)

Figure 2: Hexa Pilot Insertion

of pilot placement is beneficial. In comb pilot channel estimation, the pilot signals Np are uniformly injected into Y(k) using the following equation:

$$Y(k) = Y(mL - l) \tag{16}$$

Where L= number of subcarriers N_p and m is the pilot carrier value. The estimate of the channel at pilot subcarriers based on LS estimation is given by:

$$R_e = \frac{X_p}{Y_p}, \text{k=0, 1, … } N_p\text{-1} \tag{17}$$

Where $X_p(k)$ and $Y_p(k)$ are the output and input at the kth pilot sub-carrier respectively.

3.3.3 Hexagonal quadrature amplitude modulation type (Hexa)

Existing deep learning frameworks, such as TensorFlow, PyTorch, and Caffe, are efficient and are often updated by open-source developers to improve efficiency. Rather than developing Hexa CNN from the ground up, we built it using the Tensor Flow framework, using its core libraries and external Eigen library to preserve Hexa CNN's broad applicability. In this sense, constructing Hexa CNN models of various neural network architectures on Hexa CNN is analogous to implementing rectangle CNN models of various structures on TensorFlow. As a result, Hexa CNN serves as a foundation for developing Hexa CNN models, which are CNN models that accept hexagonal inputs directly. The tensor in TensorFlow is rectangle-shaped, hence all tensor-related procedures must be recast for hexagonal processing. TensorFlow's input is rectangular. In compared to other hexagon-imitation models, Hexa CNN saves storage space for input and filters.

Figure 3 displays the illustration of hexagonal constellations for various values of N = 8, 16, 32, 64, 128 and 256. This image illustrates how HQAM constellations might reduce transmitted power when symbol separation is present and perhaps address the energy-efficiency issue.

Typically, two integers, i and j, are used to parameterize hexagonal constellation points.

$$(x_p y_p) = \sqrt{\rho}\left((x_0, y_0) + j_p(1,0) + i_p\left(\frac{1}{2}, \frac{\sqrt{3}}{2}\right)\right) \tag{18}$$

In this case, ($d_{min} = \sqrt{\rho}$), the smallest distance between neighboring constellation points, can be used to denote $\sqrt{\rho}$. The phrase (x_0, y_0) is chosen with the goal of reducing the highest energy. Note that there is no change at all in the properties of hexagonal coordinates when they are rotated orthogonally. Additionally, the maximum energy E_{max} and the average energy E_{avg} according to the aforementioned formulas can be obtained as follows.

$$E_{avg} \triangleq \frac{\rho}{N}\sum_{p=1}^{N}\left|\left(x_0 + j_p + \frac{i_p}{2}\right), \left(y_0 + i_p\frac{\sqrt{3}}{2}\right)\right|^2 \tag{19}$$

$$E_{max} \triangleq \rho \max_p \left|\left(x_0 + j_p + \frac{i_p}{2}\right), \left(y_0 + i_p\frac{\sqrt{3}}{2}\right)\right|^2 \tag{20}$$

Where p=1,2, . . ., N, Additionally, by utilizing these expressions, a comparison between different HQAM constellation approach and traditional QAM constellations will provide a clearer understanding of the energy-efficiency of HQAM. As is commonly understood from communication theory, this point's power is expressed as $|X_p|^2 = x^2 + y^2$. Given the assumption of equal probability for each symbol in the constellation.

$$T_{avg} = \frac{1}{N}\sum_{p=1}^{N}|X_T|^2 \tag{21}$$

CFM is a metric for evaluating constellation quality. Each constellation that performs better than the other constellations is the one with the larger CFM formula is:

$$\xi = \frac{d_{min}^2}{T_{avg}} \tag{22}$$

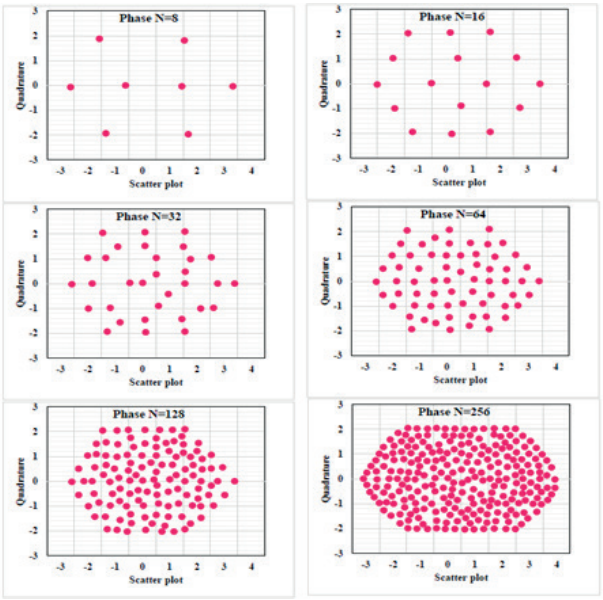

Figure 3: Hexa constellations for M = 8, 16, 64 128 and 256

3.4 Deep learning based Hexa CNN

The Hexa CNN approach improves outcomes while maintaining the same power assumption. Hexa CNN is a sort of regularized feed-forward neural network that learns feature engineering by improving filters. The adoption of regularized weights across fewer connections eliminates vanishing and expanding gradients found in previous neural networks during back propagation.

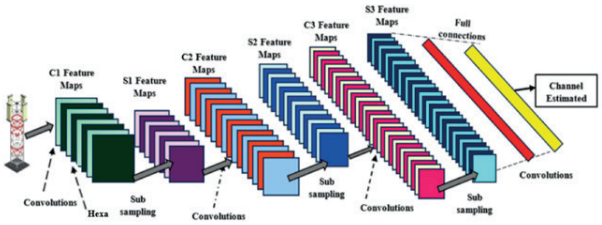

Figure 4: Architecture of Hexa CNN

As represent in Fig 4, the convolutional layer (CL) of the Hexa CNN. The data components in CV reflect channel communication, which is a two-dimensional array whereas the kernel filter. As seen in (23), the convolution filter in our proposed CNN model is effectively a 1-D mean filter:

$$\overline{a} = \frac{1}{m}\sum_{x=1}^{m} a_x \tag{23}$$

where xi represents the ith time sample and n is the total number of samples used to determine the mean.

$$N \times \left\{ \frac{\left(M - W_s\right)}{stp} + 1 \right\} \tag{24}$$

The window size (WS) is expressed (in samples). WS is set to 128 samples in this article. One second is the equivalent of this window with a sampling rate of 128.

$$5\text{trails} \times 14 \text{ channels} \times 129 \text{ averaged time samples} \tag{25}$$

The RMS value of each row's elements is extracted by the second layer, Pooling layer_1, inside a window size of WP = 64, as per equation (26):

$$A_{RMS} = \sqrt{\frac{1}{m}\sum_{x=1}^{m} a_{sx}^2} \tag{26}$$

where n represent the chosen window size, which is 64, and xci is the ith element in the convolution layer's output. Sample sizes are shrunk by a factor of 64, and the Pooling layer's output size may be expressed as follows:

$$N \times \left(M_2 - W_q\right) + 1 \tag{27}$$

where Wp is the pooling layer window size and N2 is the convolutional layer's column size. Each class's final feature matrix is 5 by 14 and is translated into a 1-D vector with 70 samples.

4 Result and discussion

In this result section evaluates and compares the performance of the proposed Hexa-QAM. The proposed HEXA-QAM was evaluated with different performance measures based on CE. For implementation, the Network Simulator (NS2) was used, which had 4-GB RAM and an Intel Core processor. Regarding, Accuracy, Recall, sensitivity, Precision and Specificity.

Table 1; Simulation parameters

Parameters	Specifications
Carrier Frequency	4 GHz
Number of active carriers	256
Pilot Ratio	64 pilots or 8 pilots
Number of subcarriers	64
Guard type	Cyclic extension
Bandwidth	17.5 kHz
Signal constellation	16QAM, BPSK
Channel Model	Rician Fading Channel
power allocation factor (PAF)	PAF are chosen as β1=0.15=15% for the user of a strong channel.
Number of subcarriers	50
cp length	16,8
learning rate	0.01
Training sample	320000

We simulate the performance of the new strategy and compare it to traditional schemes. The OFDM system parameters employed in our simulation are listed in Table 1.

4.1 Performance Metrics

The following statistical characteristics are used to analyze the classification strategy's effectiveness: accuracy, precision, specificity, sensitivity, and recall.

Figure 5 demonstrates the performance of the proposed model better than the other methods. The accuracy of the proposed technique can be as high as 99.95%, while that of traditional models like the OMA-

NOMA, MRC, PD-NOMA and UR-NOMA is 85.32, 84.9%, 87.58%, and 93.91%, respectively. The accuracy of the proposed approach improved by 14.63, 16.09%, 13.8%, and 3.75% when compared to the existing methods, respectively.

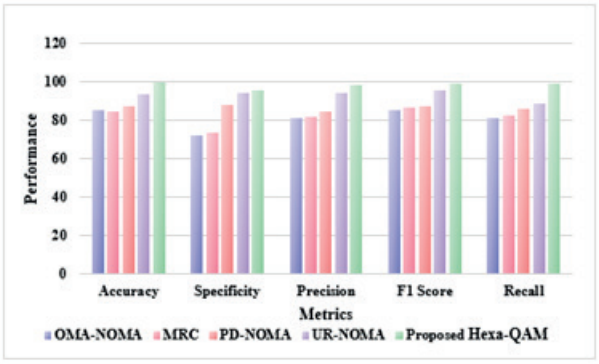

Figure 5: Performance metrics via Existing

4.2 Computational time

Table 2 compares the computation time recommended with the currently used conventional approach.

Table 2: Comparison of Computational Time

Methods	Computational Time (CT)
ANN	0.952
RNN	0.84
DNN	0.621
Proposed HEXA-QAM	0.38

The time required by the suggested approach is 0.38 seconds, whereas the computational complexity reached by the current methods is 0.952 seconds, 0.84 seconds, 0.621 seconds for ANN, RNN, and DNN, respectively. The computational time comparison reveals that the suggested Hexa CNN has less complexity than the current approaches.

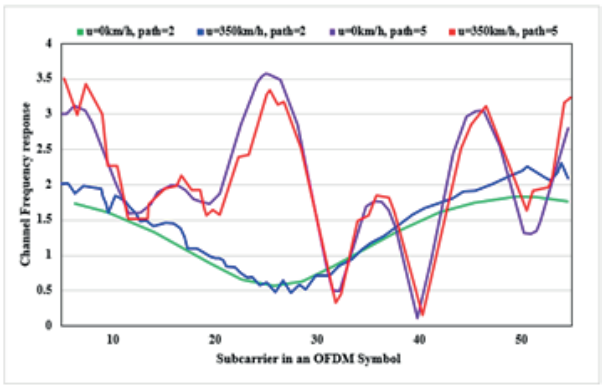

Figure 6: Channel Frequency Response

Figure 6 depicts the channel frequency response of subcarriers in an OFDM symbol at multipath numbers 2 and 6, respectively, at cellular speeds of 0 and 350 km/h. The graphic shows how multipath can produce fading in the frequency domain. Fading grows as the number of multipath pathways increases.

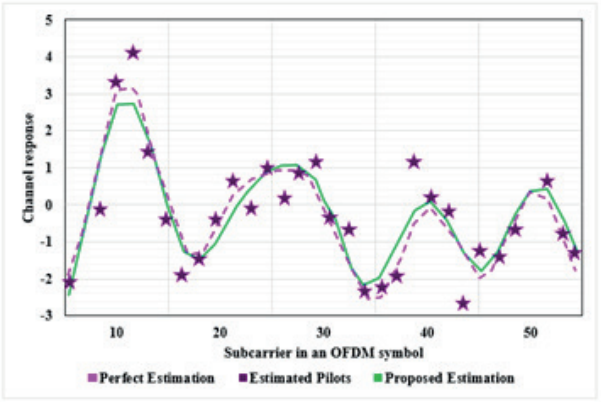

Figure 7: Sub carrier in an OFDM symbol

The suggested HEXA-QAM regression is depicted in Figure 7. Pilots are inserted in the frequency and temporal domains with insertion intervals f=2, t=2, SNR=10 dB, multipath number L=5, and travel speed v=350 km/h in this simulation experiment.

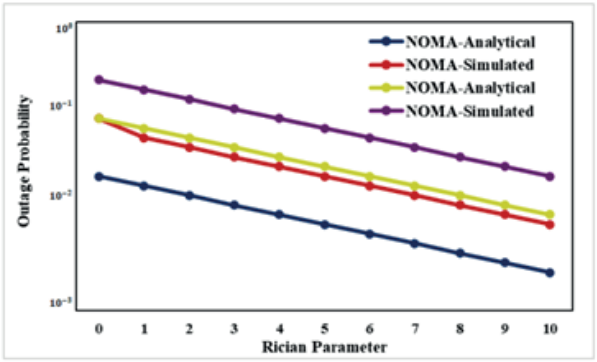

Figure 8: Rician Fading Distribution Outage Probability

The suggested HEXA-QAM can forecast the channel frequency response accurately, and its robustness is proved by its ability to overlook outliers, i.e., pilot samples with high noise. The solid line represents the suggested RICH-NOMA method interpolation, the dotted line represents the entire estimation result unaffected by simulation noise, and the asterisk represents the projected channel response at the pilot point using the LS approach.

The outage probability variation over the Rician fading distribution is seen in Fig. 8. For HEXA-QAM, the outage probability is computed based on the quantity of interfering signals. One may compute the outage prob-

ability by ranging between 1 and 10. In this case, the likelihood of an outage decreases for both users as it increases.

(a)

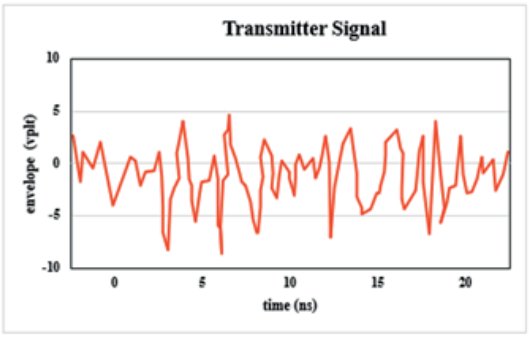

(b)

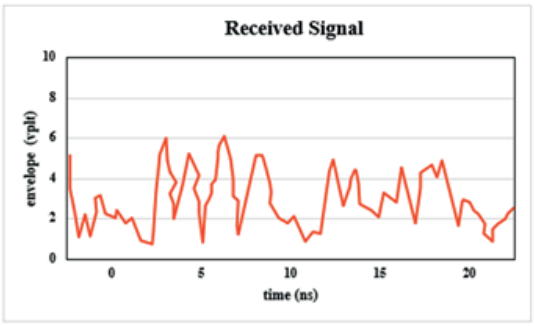

Figure 9: (a) Transmitter Signal(b) Received Signal

The two-frequency signal used to deliver the Rician Fading signal is seen in Figures 9 (a) and (b). An investigation of a simulation model for the Rician Fading channel is performed. In this scenario, the multipath signal comes at a distinct time and frequency.

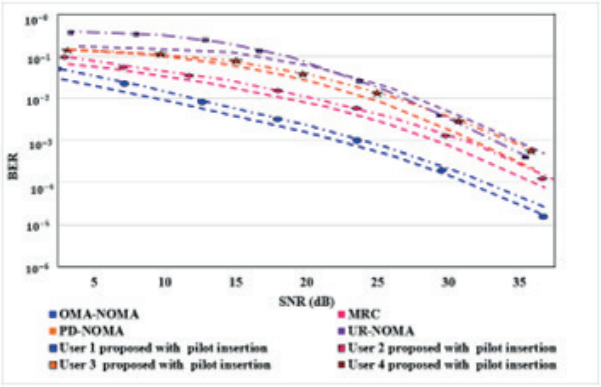

Figure 10: Block Type

This causes Rician Fading on the output side of the envelope detector. The BER performances of four-consumer HEXA-QAM with excellent pilot insertion methods are shown in Fig. 9 to underline the importance of the pilot insertion strategies. In terms of BER performance, Fig. 10 shows that the RICH-NOMA with block type insertion outperforms the existing.

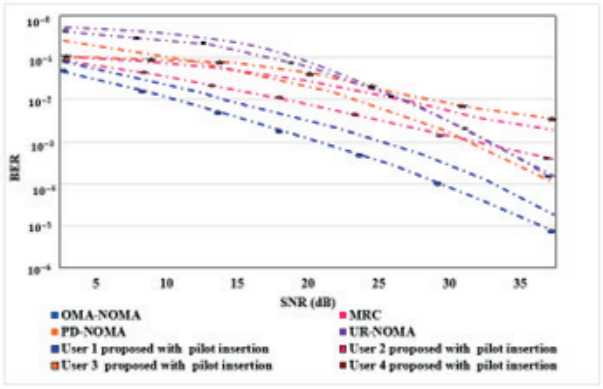

Figure 11: Comb Type

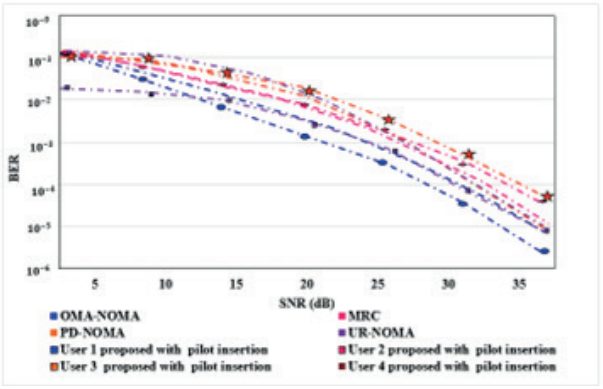

Figure 12: Hexa Type

Although it is a mixed CE and detection strategy that may outperforms the existing, the encouraged RICH-NOMA with comb-like pilot insertion outperforms it significantly Figure 11 and 12.

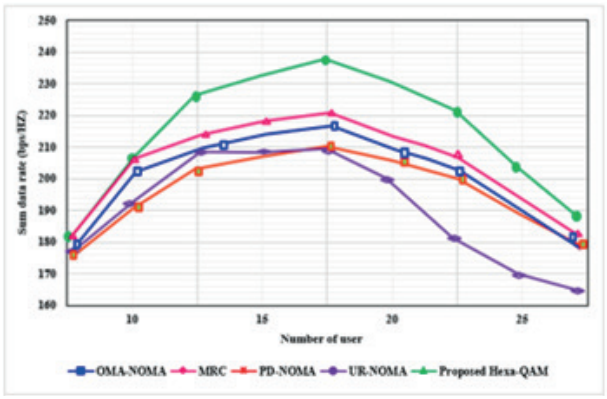

Figure 13: Sum data rate vs. number of users.

Figure 13 illustrates the potential aggregate data rate for different network systems vs the total number of users at each base station. More users at each base station result in increased intra-cell interference because of the channel's considerable route loss. However, in terms of OMA-NOMA, MRC, PD-NOMA, and UR-NOMA,

the suggested RICH-NOMA outperforms existing systems.

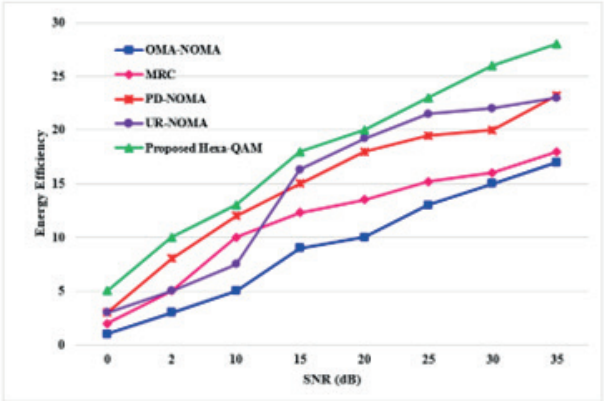

Figure 14: Energy Efficiency

As can be seen in Fig. 14, all approaches exhibit an increase in energy efficiency as SNR increases. The proposed Hexa-QAM scheme outperformed the existing OMA-NOMA, MRC, PD-NOMA, and UR-NOMA, approach in terms of EE. The EE of the proposed Hexa-QAM method is17%, 18%, 23.2%,23% and 28 % better than existing techniques.

5 Conclusions

In this paper proposed a novel Hexa CNN for NOMA Rician channel estimator using Hexagonal Quadrature Amplitude Modulation for signal detection and channel estimation (Hexa-QAM). In this proposed model contains three pilot insertion types Comp, Block, and Hexa were used in the proposed model. The proposed Hexa-QAM can detect the symbols for all users without additional operations based on pilot responses and data signals. However, Hexa CNN is used at the receiver to accomplish a joint flexible signal detection. The Hexagonal Quadrature Amplitude Modulation (Hexa CNN) achieves much better error performance than similar detectors. The proposed Hexa-QAM scheme outperformed the existing OMA-NOMA, MRC, PD-NOMA, and UR-NOMA, approach in terms of energy efficiency. The EE of the proposed Hexa-QAM technique is 17%, 18%, 23.2%, 23% and 28% better than existing techniques. The accuracy of the proposed technique can be as high as 99.95%, while that of traditional models like the OMA-NOMA, MRC, PD-NOMA and UR-NOMA is 85.32%, 84.9%, 87.58%, and 93.91%, respectively. The accuracy of the proposed approach improved by 14.63%, 16.09%, 13.8%, and 3.75% when compared to the existing methods, respectively. The proposed Hexa-QAM model has a shortcoming in that it does not account for multi-ownership. This constraint will be regarded as a future task to expand our proposed system.

The limitation of the proposed Hexa-QAM model does not handle the multi-owner nature. This limitation will be considered as a future work for extending our proposed system. In the future, we will consider employing artificial intelligence approaches to optimize each user's power allotment and improve the performance of the NOMA method.

6 Acknowledgments

The authors would like to thank the reviewers for all of their careful, constructive and insightful comments in relation to this work.

7 Conflict of Interest

The authors declare that they have no known competing financial interests or personal relationships that could have appeared to influence the work reported in this paper.

8 References

1. S. Alimi, O.D. Alao and Q.A. Mumuni, An overview of orthogonal frequency division multiplexing principles, architecture, and its application. *Global Journal of Engineering and Technology Advances*, vol.*12*, no.1, pp. 120-130 2022.
2. G.A. Abed, A New Approach to Improve Transmitting and Receiving Timing in Orthogonal Frequency Division Multiplexing (OFDM) Systems. *Iraqi Journal For Computer Science and Mathematics*, vol. *4*, no. 2, pp. 83-96, 2023.
3. A.A. Patil, C.M. Jadhao, S.S. Mhaske and R.R. Karhe, Performance Analysis of Adaptive Modulation and Coding Over AWGN Channel in an OFDM System. *International Journal of Research in Engineering, Science and Management*, vol. *6*, no.5, pp. 72-78, 2023.
4. R. Kanthavel, R. Dhaya, and A. Ahilan, AI-Based Efficient WUGS Network Channel Modeling and Clustered Cooperative Communication. ACM Transactions on Sensor Networks, vol. 18, no. 3, 2022.
5. Krishna Bikram Shah, S. Visalakshi and Ranjit Panigrahi, Seven class solid waste management-hybrid features based deep neural network, International Journal of System Design and Computing, vol. 01, no.01, pp. 1-10, 2023.
6. M. Prabhu, B. Muthu Kumar, and A. Ahilan, Slime Mould Algorithm based Fuzzy Linear CFO Estimation in Wireless Sensor Networks. IETE Journal of Research, 1-11, 2023.

7. M. Amanullakhan, M. Usha and S. Ramesh, Intrusion Detection Architecture (IDA) In IOT Based Security System, International Journal of Computer and Engineering Optimization, Vol. 01, no. 01, pp. 33-42, 2023.
8. A. Sayed, M. Khatun, T. Ahmed, A.A. Piya, P. Chakraborty and T. Choudhury, Performance analysis of OFDM system on multipath fading and inter symbol interference (ISI) using AWGN. In *Computational Intelligence in Pattern Recognition: Proceedings of CIPR 2021* Springer Singapore. pp. 25-36, 2022.
9. M.J.M. Ameen and S.S. Hreshee, Securing Physical Layer of 5G Wireless Network System over GFDM Using Linear Precoding Algorithm for Massive MIMO and Hyperchaotic QRDecomposition. *International Journal of Intelligent Engineering & Systems*, vol. *15*, no. 5, 2022.
10. K.S. Ali, E. Hossain and M.J. Hossain, Partial non-orthogonal multiple access (NOMA) in downlink poisson networks. *IEEE Transactions on Wireless Communications*, vol. *19*, no. 11, pp. 7637-7652, 2020.
11. M. F. Zia, and J. M. Hamamreh, An Advanced Non-Orthogonal Multiple Access Security Technique for Future Wireless Communication Networks. RS Open Journal on Innovative Communication Technologies, vol. 1, no. 2, 2020.
12. M. Abewa, and J. M. Hamamreh, Multi-User Auxiliary Signal Superposition Transmission (MU-AS-ST) for Secure and Low-Complexity Multiple Access Communications. RS Open Journal on Innovative Communication Technologies, vol. 2, no. 4, 2021.
13. M. F. Zia, H. M. Furqan, and J. M. Hamamreh, Multi-cell, Multi-user, and Multi-carrier Secure Communication Using Non-Orthogonal Signals' Superposition with Dual-Transmission for IoT in 6G and Beyond. RS Open Journal on Innovative Communication Technologies, vol. 2, no. 3, 2021.
14. J. M. Hamamreh, M. Abewa, and J. P. Lemayian, New Non-Orthogonal Transmission Schemes for Achieving Highly Efficient, Reliable, and Secure Multi-User Communications. RS Open Journal on Innovative Communication Technologies, vol. 1, no. 2, 2020.
15. M. Hadi and R. Ghazizadeh, Joint sub-carrier allocation and 3D beamforming design in OMA-NOMA based mmWave heterogeneous networks under channel uncertainties. *AEU-International Journal of Electronics and Communications*, vol. *137*, pp. 153809, 2021.
16. F. Rahdari, N. Movahhedinia, M.R. Khayyambashi and S. Valaee, QoE-aware power control and user grouping in Cognitive Radio OFDM–NOMA systems. *Computer Networks*, vol. 189, pp. 107906, 2021.
17. B.E.Y. Belmekki, A. Hamza and B. Escrig, On the performance of cooperative NOMA Using MRC at road intersections in the presence of interference. *Physical Communication*, vol. 46 pp. 101321, 2021.
18. L.T. Anh and H.Y. Kong, Multi-User PD-NOMA with unreliable backhaul links in a multiple EH relay network over Nakagami-m fading channels. *Physical Communication*, vol. 47, pp. 101351, 2021.
19. F. Cogen and E. Aydin. Performance analysis of Hexagonal QAM constellations on quadrature spatial modulation with perfect and imperfect channel estimation. *Physical Communication*, vol. 47, pp. 10137, 2021.
20. Y. Tian, B. Xiao, X. Wang, Y.H. Kho and C. Tian, Performance analysis of opportunistic NOMA strategy in uplink coordinated multi-points systems. *Computer Communications*, vol. 177 pp. 207-212, 2021.
21. M. Kazemian, J. Abouei and A. Anpalagan, A low complexity enhanced-NOMA scheme to reduce inter-user interference, BER and PAPR in 5G wireless systems. *Physical Communication*, vol. 48 , pp. 101412, 2021.
22. M. Ghous, A.K. Hassan, Z.H. Abbas and G. Abbas, Modeling and analysis of self-interference impaired two-user cooperative MIMO-NOMA system. *Physical Communication*, vol. 48, pp. 101441, 2021.
23. Z. Wang, S. Wei, L. Zou, F. Liao, W. Lang and Y. Li, Deep-Learning-Based Carrier Frequency Offset Estimation and Its Cross-Evaluation in Multiple-Channel Models. *Information*, vol. 14, no. 2, pp. 98, 2023.
24. J. P. Lemayian, and J. M. Hamamreh, A Novel Small-Scale Nonorthogonal Communication Technique Using Auxiliary Signal Superposition with Enhanced Security for Future Wireless Networks. RS Open Journal on Innovative Communication Technologies, vol. 1, no. 2, 2020.

Arrived: 22. 11. 2023
Accepted: 03. 03. 2024